Eidgenössische Technische Hochschule Zürich

Ecole polytechnique fédérale de Zurich
Politecnico federale di Zurigo
Swiss Federal Institute of Technology Zurich

Fast numerical solution of the linearized Molodensky problem*

R. Klees**, M. van Gelderen**, C. Lage† and C. Schwab

Research Report No. 99-16
September 1999

Seminar für Angewandte Mathematik
Eidgenössische Technische Hochschule
CH-8092 Zürich
Switzerland

*This research is supported in part by the TMR Project "Wavelets and Multiscale Methods" through the Swiss Federal Office for Education and Science under Contract No. BBW 97.0404

**Delft Institute for Earth-Oriented Space Research (DEOS), Faculty of Civil Engineering and Geosciences, Delft University of Technology, 2629 JA Delft, The Netherlands

†Coyote Systems, 2740 Van Ness Ave #210, San Francisco, CA 94109, USA

Fast numerical solution of the linearized Molodensky problem*

R. Klees**, M. van Gelderen**, C. Lage† and C. Schwab

Seminar für Angewandte Mathematik
Eidgenössische Technische Hochschule
CH-8092 Zürich
Switzerland

Research Report No. 99-16 September 1999

Abstract

When *standard* boundary element methods (BEM) are used to solve the linearized vector Molodensky problem we are confronted with two problems: (i) the absence of $O(|x|^{-2})$ terms in the decay condition is not taken into account, since the single layer ansatz, which is commonly used as representation of the perturbation potential, is of the order $O(|x|^{-1})$ as $x \to \infty$. This implies that the standard theory of Galerkin BEM is not applicable since the injectivity of the integral operator fails; (ii) the $N \times N$ BEM stiffness matrix is dense, with N typically of the order 10^5. Without fast algorithms, which provide suitable approximations to the stiffness matrix by a sparse one with $O(N(\log N)^s),\ s \geq 0$, non-zero elements, high-resolution global gravity field recovery is not feasible.

We propose solutions to both problems. (i) A proper variational formulation taking the decay condition into account is based on some closed subspace of co-dimension 3 of $L^2(\Gamma)$. Instead of imposing the constraints directly on the boundary element trial space, we incorporate them into a variational formulation by penalization with a Lagrange multiplier. The conforming discretization yields an augmented linear system of equations of dimension $N + 3 \times N + 3$. The penalty term guarantees the well-posedness of the problem, and gives precise information about the incompatibility of the data. (ii) Since the upper left submatrix of dimension $N \times N$ of the augmented system is the stiffness matrix of the standard BEM, the approach allows to use all techniques to generate sparse approximations to the stiffness matrix such as wavelets, fast multipole methods, panel clustering etc. without any modification. We use a combination of panel clustering and fast multipole method in order to solve the augmented linear system of equations in $O(N)$ operations.

In order to demonstrate the potential of the method we solve a Robin problem on the sphere with a nullspace of dimension 3. For $N = 65538$ unknowns the matrix assembly takes about 600 s and the solution of the sparse linear system using GMRES without any preconditioning takes about 8 s on a workstation. 30 GMRES iterations are sufficient to make the error smaller than the discretization error.

*This research is supported in part by the TMR Project "Wavelets and Multiscale Methods" through the Swiss Federal Office for Education and Science under Contract No. BBW 97.0404

**Delft Institute for Earth-Oriented Space Research (DEOS), Faculty of Civil Engineering and Geosciences, Delft University of Technology, 2629 JA Delft, The Netherlands

†Coyote Systems, 2740 Van Ness Ave #210, San Francisco, CA 94109, USA

1 Introduction

The determination of the exterior gravity field of the Earth from terrestrial observations is usually formulated in terms of a boundary value problem (BVP) for the Laplace-Poisson equation. Depending on the type of observations several boundary value problems can be defined. However, after linearization around a suitable approximate solution all problems are more or less special cases of the exterior oblique derivative BVP for the Laplace operator; the boundary surface is either the Earth's surface, a suitable approximation to it like a telluroid or an ellipsoid of revolution. Numerical solutions of the linearized BVP are usually based on various additional approximation steps like, e.g., spherical approximation and constant radius approximation.

Here we consider Galerkin methods for integral equation formulations of the linearized BVP which avoid any of the aforementioned approximations. The price to pay for this is that the kernel functions are non-isotropic and the boundary surface is non-spherical. Therefore, the assembly of the linear system of equations becomes more elaborate; moreover, since the system matrix is dense, sparse solvers cannot be used any more to solve for the huge number of unknowns.

There is another aspect which has to be taken into account in the formulation of geodetic BVPs. Usually, the low frequency components of the geopotential are accurately obtained by satellite measurements. That means that a number of coefficients in the spherical harmonics series expansion of the geopotential is determined with a precision that cannot be improved by terrestrial data. This is accounted for in the formulation of the geodetic BVP in the form of additional constraints to the perturbation problem. The same holds if the geodetic BVP lacks well-posedness. For instance, the vector Molodensky BVP requires the first order terms in the expansion of the geopotential in spherical harmonics to vanish in order to ensure uniqueness of the solution; for the same reason the Altimetry-Gravimetry I & II BVPs require that no zero order term is present. Finally, if the measured data is not in the range of the operator the problem may even not have any solution at all.

Therefore, a numerical approach has to be designed that can handle these peculiarities of geodetic BVPs. As far as Galerkin methods to integral equations are concerned this implies the following questions: (i) how to properly handle the conditions that ensure well-posedness of the problem, (ii) how to properly include satellite-derived geopotential models, and (iii) how to design a fast algorithm which is suitable for high resolution global geopotential recovery with a performance that is almost independent of (i) and (ii)?

Our solution to (i) and (ii) is based on a new saddle point formulation which avoids to modify the trial and test spaces. The solution to (iii) is a fast algorithm that combines

ideas of panel clustering and fast multipole methods, and which is easy to combine with the saddle point formulation.

2 The mathematical model

The linearized Molodensky problem reads as follows: Given a differentiable embedding $\varphi : S^2 \to \mathbb{R}^3$ and a function f on the surface $\Gamma := \partial\varphi(S^2) \subset \mathbb{R}^3$: find $U(x)$ satisfying

$$\triangle U(x) = 0 \qquad x \in \text{ext } \Gamma\,, \tag{2.1a}$$

$$U(x) + \langle \nabla U(x), h(x)\rangle = f(x) \qquad x \in \Gamma\,, \tag{2.1b}$$

$$U(x) = \frac{c}{|x|} + O(|x|^{-3}), \quad |x| \to \infty\,, \quad c \in \mathbb{R}\backslash\{0\}\,. \tag{2.1c}$$

Under certain conditions on $\varphi(x)$ and the field $h(x)$, which we shall assume to hold in what follows, (2.1) is a regular oblique derivative problem, and Fredholm's alternative holds. It was proved in [5] that the homogeneous problem (2.1) is uniquely solvable, while the homogeneous problem (2.1a), (2.1b) admits 3 eigensolutions which span the nullspace $\mathcal{N}$. Thus, uniqueness implies existence, and the former requires that the data f satisfies 3 compatibility conditions, i.e., the data f must be orthogonal to the nullspace of the homogeneous adjoint BVP which, due to Fredholm's alternative, has dimension 3 as well. Moreover, the problem has a unique solution $U \perp \mathcal{N}$ if f satisfies this compatibility condition.

In order to reformulate the BVP (2.1) as an integral equation, we satisfy the differential equation (2.1a) by the single layer ansatz with kernel $k(z) = (4\pi|z|)^{-1}$:

$$U(x) = \int_{y\in\Gamma} k(x-y)\, u(y)\, d\Gamma(y), \quad x \in \text{ext } \Gamma \tag{2.2}$$

where u is the unknown density function. Inserting (2.2) into the boundary condition (2.1b) yields a Cauchy singular boundary integral equation for the unknown density u:

$$\begin{aligned} Au := -\frac{h(x)\cdot n(x)}{2}\, u(x) \;&-\; \int_\Gamma h(x)\cdot\nabla_x\, k(x-y)u(y)d\Gamma(y) \\ &+\; \int_\Gamma k(x-y)u(y)d\Gamma(y) = f(x), \quad x \in \Gamma \end{aligned} \tag{2.3}$$

If the field $h(x)$ does not deviate too much from the exterior unit normal vector $n(x)$ to Γ, the principal symbol of the integral operator A is positive which implies that A is strongly elliptic. Moreover, we assume that A is bijective from $L^2(\Gamma) \to L^2(\Gamma)$ (this assumption could be weakened). Notice, however, that the absence of the $O(|x|^{-2})$-terms in the decay condition (2.1c) is not taken into account by (2.2) since the single layer potential is of order $O(|x|^{-1})$ as $|x| \to \infty$.

3 Weak formulation and Galerkin approximation

We use the Galerkin method in order to discretize the boundary integral equation (2.3). Note that we could use collocation as well, but this would not be the proper discretization method for the linearized geodetic BVPs, where we usually have to deal with Cauchy-singular and hypersingular operators A. We consider the weak form of the integral equation (2.3):

$$u \in L^2(\Gamma): \qquad \langle Au, v\rangle = \langle f, v\rangle \quad \forall v \in L^2(\Gamma), \tag{3.1}$$

where $\langle\cdot,\cdot\rangle$ denotes the $L^2(\Gamma)$-inner product. The Galerkin method in abstract form reads: Given a dense sequence $\{V_N\}_{N=0}^{\infty}$ of finite dimensional subspaces of $L^2(\Gamma)$, find

$$u_N \in V_N: \qquad \langle Au_N, v\rangle = \langle f, v\rangle \quad \forall v \in V_N. \tag{3.2}$$

Hence, for a given basis $\{b_1, \ldots, b_N\}$ of V_N, we have to solve the linear system of equations $\mathbf{Au} = \mathbf{f}$ where the stiffness matrix $\mathbf{A}$ and the right-hand side $\mathbf{f}$ are defined by

$$(\mathbf{A})_{ij} := \langle b_i, Ab_j\rangle, \text{ and } (\mathbf{f})_i := \langle b_i, f\rangle, \quad i, j = 1 \ldots N. \tag{3.3}$$

It is known that continuity, Garding inequality, and injectivity of the operator A ensure the unique solvability of this system, provided that N is sufficiently large [4]. However, in our case (3.1) does not take into account the constraint $U \perp \mathcal{N}$ which means that U resp. U_N computed from u resp. u_N via (2.2) will violate (2.1c). The *proper* weak formulation of $Au = f$ must not be based on $L^2(\Gamma)$ but on some closed subspace of co-dimension 3 of $L^2(\Gamma)$:

$$u \in L^2(\Gamma) \cap \mathcal{N}^{\perp}: \qquad \langle Au, v\rangle = \langle f, v\rangle \quad \forall v \in L^2(\Gamma) \cap \mathcal{N}^{\perp} \tag{3.4}$$

The corresponding conforming approximate solution is

$$u_N \in V_N \cap \mathcal{N}^{\perp}: \qquad \langle Au_N, v\rangle = \langle f, v\rangle \quad \forall v \in V_N \cap \mathcal{N}^{\perp} \tag{3.5}$$

Therefore, we need the subspace $\mathcal{N}$. In our case the condition of vanishing $O(|x|^{-2})$-terms in the expansion of U at infinity is equivalent to the orthogonality of the density u to the restriction to the boundary Γ of the homogeneous harmonic polynomials of degree 1 (for a proof we refer to Appendix A). This implies that $\mathcal{N}$ in (3.4), (3.5) is the linear space spanned by the restriction to the boundary Γ of the 3 homogeneous harmonic polynomials of degree 1:

$$\mathcal{N} = \text{span}\{\, H_{1,m}|_{\Gamma} : m = -1, 0, 1\} \tag{3.6}$$

4 The saddle point formulation

The conforming Galerkin discretization (3.5) is difficult to realize in practice. The reason is that the homogeneous harmonic polynomials of degree 1 which span $\mathcal{N}$ are globally

supported, and for the computations a basis of $V_N \cap \mathcal{N}^\perp$ must be generated. Since the dimension of V_N is typically very large (in the experiments below about 10^5 gravity field parameters have to be solved for), it is a non-trivial matter how to do that stably and efficiently. Moreover, the support of the base functions spanning $V_N \cap \mathcal{N}^\perp$ will be larger than the support of the base functions spanning V_N which increases the computational effort. [6] have discussed this problem in another context, and have proposed the method of modified multiscale trial & test spaces. However, this solution strategy is currently limited to constraints involving homogeneous harmonic polynomials of degree 0.

Here, we propose a different approach: We reformulate (3.4) as a *saddle point problem* analogous to what is done in incompressible fluid flow. The constraint $u \perp \mathcal{N}$ will not be imposed directly on the boundary element space V_N, but will rather be incorporated into the variational formulation by penalization with a Lagrange multiplier p. This leads to an augmented system which reads:

$$(u,p) \in L^2(\Gamma) \times \mathcal{N}: \qquad \begin{array}{lcll} \langle Au, v\rangle + \langle Ap, v\rangle & = & \langle f, v\rangle & \forall v \in L^2(\Gamma) \\ \langle u, q\rangle & = & 0 & \forall q \in \mathcal{N} \end{array} \tag{4.1}$$

and the conforming Galerkin approximation to (4.1) is:

$$(u_N,p_N) \in V_N \times \mathcal{N}: \qquad \begin{array}{lcll} \langle Au_N, v\rangle + \langle Ap_N, v\rangle & = & \langle f, v\rangle & \forall v \in V_N \\ \langle u_N, q\rangle & = & 0 & \forall q \in \mathcal{N} \end{array} \tag{4.2}$$

(u,p) is called the saddle point of the variational system. The conforming approximation defines a linear system of equations of dimension $N+3$. The upper left matrix is the usual $N \times N$ stiffness matrix of the unconstrained problem, the upper right and the transposed of the lower left matrix have dimension $N \times 3$; their elements are inner products of the bases of $A\mathcal{N}$ and of $\mathcal{N}$, respectively, with the basis of V_N.

A major advantage of the saddle point formulation is that all techniques to generate sparse approximations to the matrix $\langle Au_N, v\rangle$ such as wavelets, fast multipole methods, panel clustering etc. can be used here without any modification. Moreover, if the data happen to be compatible, then, of course, $p = 0$. In practice, however, f is not exactly compatible due to various data and approximation errors. Then, the saddle point formulation (4.1) is still well-posed and the size of p gives precise information about the degree of incompatibility of the data f. Note that the proper weak formulation (3.4) would not have a solution if f were incompatible.

Remark 4.1 The assembly of the matrix $\langle Ap_N, v\rangle$ is of order $O(N^2)$. In particular, if $\mathcal{N} \subset V_N$ the assembly process consists of three matrix vector multiplications with the stiffness matrix $\mathbf{A}$. However, fast cluster algorithms as proposed in Section 6 could be used to reduce the complexity of the calculations substantially. The assembly of $\langle u_N, q\rangle$ takes $O(N)$ operations, and therefore, does not make the numerics much more elaborate.

5 Convergence Analysis

We set $V = L^2(\Gamma)$ in what follows and note that the operator A in (2.3) as well as its adjoint A^* are bounded, linear operators on V: for all $v \in V$ holds

$$\|Av\|_V \leq C\,\|v\|_V, \quad \|A^*v\|_V \leq C^*\|v\|_V\,. \tag{5.1}$$

Further, A satisfies a Gårding inequality: there exists $\gamma > 0$ and a compact operator K on $V = L^2(\Gamma)$ such that

$$\forall v \in V: \quad \langle v, (A+K)v\rangle \geq \gamma\,\|v\|_V^2\,. \tag{5.2}$$

Lemma 5.1 *Let $A : V \to V$ be bounded, injective and assume that (5.2) holds. Let $\{V_N\}_N$ be a dense sequence of subspaces of V. Then there exist $N_0 \in \mathbb{N}$, $\gamma_0 > 0$ such that for every $N \geq N_0$ holds the discrete inf-sup condition:*

$$\inf_{0\neq u\in V_N} \sup_{0\neq v\in V_N} \frac{\langle Au, v\rangle}{\|u\|_V\,\|v\|_V} \geq \gamma_0\,. \tag{5.3}$$

Proof. We proceed in 3 steps.

i) The Gårding inequality (5.2) implies the continuous inf-sup condition, i.e. (5.3) with V_N replaced by V. For, given $u \in V$, select $v_u \in V$ to be a solution of $A^*v_u = u$. Then v_u exists and is unique, since A^* is injective (as is A), and by (5.1)

$$\|v_u\|_{L^2(\Gamma)} = \|(A^*)^{-1}u\|_V \leq c\,\|u\|_V\,.$$

Further,

$$\langle Au, v_u\rangle = \langle u, A^*v_u\rangle = \|u\|_V^2\,,$$

whence

$$\inf_{0\neq u\in V} \sup_{0\neq v\in V} \frac{\langle Au, v\rangle}{\|u\|_V\,\|v\|_N} \geq \frac{1}{c} > 0\,. \tag{5.4}$$

ii) We set $D = A + K$, K a compact operator on V as in (5.2). We claim that

$$\|P_N\,Au\|_V \geq \gamma_0\|u\|_V \text{ for all } u \in V,\ N \geq N_0\,,$$

where $P_N : V \to V_N$ denotes the $L^2(\Gamma)$-projection. If it were wrong, there would be a sequence $\{u_i\}_i \subset V$, $u_i \in V_i$, $\|u_i\|_V = 1$ such that

$$\|P_i\,Au_i\|_V = \|P_i\,Du_i - P_i\,K\,u_i\|_V \to 0 \quad i \to \infty\,. \tag{5.5}$$

Now, $\{u_i\}_i$ contains a weakly convergent subsequence, again denoted by u_i, i.e. $u_i \underset{V}{\rightharpoonup} u \in V$.

Now, $P_i\, Au \underset{V}{\rightharpoonup} Au$, since for every $v \in V$

$$\langle P_i\, Au_i, v\rangle = \langle u_i, A^* P_i v\rangle \to \langle u, A^* v\rangle = \langle Au, v\rangle$$

by the density of $\{V_i\}_i$ in V. Hence (5.5) implies that $Au \underset{V}{\to} 0$. Further, since K is compact, $Ku_i \underset{V}{\to} Ku$ and $P_i\, Ku_i \underset{V}{\to} Ku$. By (5.5) therefore

$$P_i\, Du_i \underset{V}{\to} Ku\,.$$

By (5.2) then

$$\begin{aligned}
\gamma\, \|u - u_i\|_V^2 &\leq |\, \langle u - u_i,\, D(u - u_i)\rangle\,| \\
&= |\, \langle D^* u, u - u_i\rangle - \langle u_i, Du\rangle + \langle u_i,\, P_i\, Du_i\rangle\,| \\
&\underset{i\to\infty}{\longrightarrow} |\, \langle u,\, Ku\rangle - \langle u, Du\rangle\,| \\
&= |\, \langle u, Au\rangle\,| \\
&= 0
\end{aligned}$$

since $Au = 0$, hence $u_i \underset{V}{\to} u$. But $\|u\|_V = 1$, since

$$\big|\, \|u_i\|_V - \|u\|_V\big| \leq \|u - u_i\|_V \to 0\,,$$

so that $u \neq 0$, and $Au = 0$, a contradiction to the injectivity of A.

iii) Proof of (5.3). Hence, for $N \geq N_0$, and every $0 \neq u \in V$,

$$\begin{aligned}
0 < \gamma_0\, \|u\|_V &\leq \|P_N\, Au\|_V = \sup_{0\neq v\in V} \frac{\langle v, P_N\, Au\rangle}{\|v\|_V} \\
&\leq \sup_{0\neq v\in V} \frac{\langle P_N v, Au\rangle}{\|P_N v\|_V}\,,
\end{aligned}$$

since $\|P_N v\|_V \leq \|v\|_V$ for every $v \in V$.

Since $V_N \subset V$, we may choose in particular any $0 \neq u = u_N \in V_N$ so that

$$0 < \gamma_0\, \|u_N\|_V \leq \sup_{v\in V} \frac{\langle P_N v, Au_N\rangle}{\|P_N v\|_V} = \sup_{v_N\in V_N} \frac{\langle v_N, Au_N\rangle}{\|v_N\|_V}\,.$$

Since $0 \neq u_N \in V_N$ was arbitrary, the discrete inf-sup condition (5.3) follows. □

We now turn to the analysis of (4.1), (4.2). To this end, we define the bilinear form $B : (V,\mathcal{N}) \times (V,\mathcal{N}) \to \mathbb{R}$ by

$$B(u,p;\, v,q) := \langle Au, v\rangle + \langle Ap, v\rangle + \langle u, q\rangle \,. \tag{5.6}$$

Unique solvability of (4.1) and (4.2) and quasioptimal convergence of u_N, p_N in (4.2) to u, resp. to p follow from inf-sup conditions for B. We have

Lemma 5.2 *The bilinear form B satisfies the inf-sup condition on $(V,\mathcal{N}) \times (V,\mathcal{N})$.*

Proof. We observe that by (5.4), A is invertible on V. Given $(u,p) \in (V,\mathcal{N})$, we select

$$q = -2p \in \mathcal{N}, \;\; v := (A^{-1})^*(u+p) \in V \,.$$

Then

$$\begin{aligned} B(u,p;\, v,q) &= \langle A(u+p), v\rangle + \langle u, q\rangle \\ &= \langle A(u+p), (A^{-1})^*(u+p)\rangle - 2\langle u, p\rangle \\ &= \|u\|_V^2 + \|p\|_V^2 = |||(u,p)|||^2 \,, \end{aligned} \tag{5.7}$$

and evidently

$$|||(v,q)||| \le C\, |||(u,p)||| \,. \tag{5.8}$$

□

The discrete inf-sup condition will now follow by a perturbation argument. For $(u,p) \in (V,\mathcal{N})$, we define $|||(u,p)||| := (\|u\|_V^2 + \|p\|_V^2)^{1/2}$. The there holds

Proposition 5.3 *Let $\{V_N\}_N$ be dense in V and $\{0\} \neq \mathcal{N} \subset V$ be finite dimensional. Define*

$$\varphi(N) := \sup_{0\neq p\in\mathcal{N}} \inf_{p_N\in V_N} \frac{\|p - p_N\|_V}{\|p\|_V} \,.$$

Then there holds for all $N \ge N_0$.

$$\inf_{\substack{u\in V_N\\ p\in\mathcal{N}}} \inf_{\substack{v\in V_N\\ q\in\mathcal{N}}} \frac{B(u,p;\, v,q)}{|||(u,p)|||\;|||(v,q)|||} \ge \gamma_0 > 0 \tag{5.9}$$

provided N_0 is such that $\varphi(N_0)$ is sufficiently small.

Proof. Let $(u_N,p) \in (V_N,\mathcal{N})$ be given, $\|u_N\|_V^2 + \|p\|_V^2 > 0$. Then, for N large enough, A is invertible on V_N by Lemma 5.1, and (5.3′) holds.

We select $q = -2p \in \mathcal{N}$ and $v_N \in V_N$ to be the solution of

$$\forall w \in V_N : \langle w, A^* v_N \rangle = \langle w, u_N + p \rangle \ . \tag{5.10}$$

By Lemma 5.1, applied to A^*, v_N exists and

$$\|v_N\|_V \le C \, |||(u_N, p)||| \le C(\|u_N\|_V + \|p\|_V) \ . \tag{5.11}$$

Pick in (5.10) $w = u_N + P_N \, p \in V_N$, and set $p_N = P_N p$. Then

$$\langle u_N + p_N, u_N + p \rangle = \langle w, A^* v_N \rangle = \langle u_N + p_N, u_N + p \rangle \ .$$

Now

$$\begin{aligned}
B(u_N, p;\, v_N, q) &= \langle A(u_N + p), v_N \rangle + \langle u_N, q \rangle \\
&= \langle A(u_N + p_N), v_N \rangle + \langle A(p - p_N), v_N \rangle + \langle u_N, q \rangle \\
&\overset{(5.10)}{=} \langle u_N + p_N, u_N + p \rangle + \langle p - p_N, A^* v_N \rangle - 2\langle u_N, p \rangle \\
&= \|u_N + p\|_V^2 - 2\langle u_N, p \rangle \\
&+ \langle p - p_N, A^* v_N \rangle + \langle p_N - p, u_N + p \rangle \\
&\ge |||(u_N, p)|||^2 - \|p - p_N\|_V (|||A^*||| \ \|v_N\|_V + \sqrt{2} |||(u_N, p)|||) \\
&\overset{(5.11)}{\ge} |||(u_N, p)|||^2 - \frac{\|p - p_N\|_V}{\|p\|_V} \sqrt{2}(1 + C \, |||A^*|||) \, |||(u_N, p)||| \ \|p\|_V \\
&\ge (1 - \varphi(N)\sqrt{2}(1 + C \, |||A^*|||)) \, |||(u_N, p)|||^2
\end{aligned}$$

from where the assertion follows. □

Remark 5.4 The condition that $\varphi(N_0)$ is sufficiently small means that V_N has to be so large as to be able to represent elements of $\mathcal{N}$ as well. If $\mathcal{N}$ consists, as it is the case in the linearized Molodensky problem, just of a few low degree spherical harmonics, this is rather easy to achieve. If, however, $\mathcal{N}$ contains a rather high order approximation of the geopotential (e.g. a spherical harmonics expansion up to order 512) then N has to be rather large. Nevertheless, even then the approach (5.10), (5.11) may be advantageous since V_N allows for local refinement on Γ, whereas spherical harmonics expansions don't.

Remark 5.5 From (5.9) follows the quasioptimal convergence of (u_N, p) in (4.2), if $\{V_N\}_N$ is dense in V since

$$\|u - u_N\|_V + \|p - p_N\|_V \le C \inf_{\substack{v \in V_N \\ q \in \mathcal{N}}} \{\|u - v\|_V + \|p - q\|_V\} \ .$$

In particular therefore $\|u - u_N\|_V \to 0$ as $N \to \infty$.

Remark 5.6 So far, we analyzed only the Galerkin scheme (5.11), where $\langle Au_N, v_N\rangle$ is realized exactly for $u_N, v_N \in V_N$. In practice, however, and in particular in the fast algorithms presented below, the interactions $\langle Au_N, v_N\rangle$ will only be available approximately, thereby introducing additional errors. The impact of these consistency errors on the Galerkin scheme (5.11) remain yet to be analyzed. In the unconstrained case, these errors do not spoil the convergence rate (e.g. [13]).

6 The fast clustering algorithm

In BEM the stiffness matrix is a dense $N \times N$-matrix, since the kernel function $k(x-y)$ links every point $x \in \Gamma$ to every point $y \in \Gamma$. Hence, storage and time consumptions of the method are of order $O(N^2)$ provided that iterative solvers could be applied efficiently which limits the application of BEM in practice. In the eighties Hackbusch and Nowak [3] developed the panel clustering method in order to overcome this grave drawback. Independently, Rokhlin proposed the fast multipole method [12]. Both methods are based on an approximation of the kernel factorizing the x, y-dependency. By this, the x-integration is separated from the y-integration reducing the amount of work substantially. More recently, Rathsfeld [11] proposed a wavelet-type basis to reduce the computational work. See also [13].

In our approach, we use a blend of panel clustering and fast multipole method. Suppose that the kernel k may be replaced by a degenerate kernel k_m

$$k(x,y) \approx k_m(x,y;x_0,y_0) = \sum_{(\mu,\nu)\in\mathcal{I}_m} \kappa_{\mu\nu}(x_0,y_0) X_\mu(x;x_0) Y_\nu(y;y_0) \tag{6.1}$$

with parameters $m \in \mathbb{N}$, $x_0, y_0 \in \mathbb{R}^3$ such that the error bound

$$|k(x,y) - k_m(x,y;x_0,y_0)| \le C_\eta\, \eta^m\, |k(x,y)| \tag{6.2}$$

is valid for some $0 < \eta < 1$ and all $x, y \in \mathbb{R}^3$ satisfying

$$|y - y_0| + |x - x_0| \le \eta\, |y_0 - x_0|. \tag{6.3}$$

Here, $\mathcal{I}_m$ denotes a finite index set.

There are several possibilities to choose an approximation by degenerate kernels [8]. In our experiments described in Section 7 approximation (6.1) was obtained by applying a truncated multipole expansion, i.e.,

$$\mathcal{J}_m := \{\mu \in \mathbb{N}_0 \times \mathbb{Z} : |\mu_2| \leq \mu_1,\, \mu_1 < m\}, \quad \mathcal{I}_m := \{(\mu,\nu) \in (\mathcal{J}_m)^2 : \mu_1 + \nu_1 < m\} \tag{6.4}$$

$$\kappa_{\mu\nu}(x_0, y_0) := \kappa_{\mu+\nu}(x_0, y_0) := \frac{1}{4\pi\, C_{\mu_1+\nu_1}^{\mu_2+\nu_2} |y_0 - x_0|^{\mu_1+\nu_1+1}}\, Y_{\mu_1+\nu_1}^{\mu_2+\nu_2}\left(\frac{y_0 - x_0}{|y_0 - x_0|}\right) \tag{6.5}$$

$$X_\mu(x; x_0) := C_{\mu_1}^{\mu_2} |x - x_0|^{\mu_1} Y_{\mu_1}^{-\mu_2}\left(\frac{x - x_0}{|x - x_0|}\right), \quad Y_\nu(y; y_0) := X_\nu(-y; -y_0) \tag{6.6}$$

with

$$C_l^p := \frac{i^{|p|}}{\sqrt{(l-p)!(l+p)!}}, \quad Y_l^p(x) := P_l^{|p|}(\cos\theta)\, \mathrm{e}^{ip\phi} \tag{6.7}$$

for $x = (\cos\phi \sin\theta, \sin\phi \sin\theta, \cos\theta)^T \in S^2$. The functions X_μ and Y_ν are solid spherical harmonics of positive degree whereas the expansion coefficients $\kappa_{\mu\nu}$ are homogeneous harmonic polynomials of negative degree. Note that the multipole expansion is nothing else but an efficient representation of the Taylor expansion of $|y-x|^{-1}$. While for arbitrary kernel functions k, the index set $\mathcal{J}_m$ of a truncated Taylor expansion contains $O(m^3)$ indices, only $O(m^2)$ coefficients must be stored to evaluate the Taylor expansion of $|y-x|^{-1}$ using the multipole ansatz according to (6.4)-(6.6). The expansion for the adjoint kernel of the double layer potential is obtained from (6.4)-(6.6) by applying the $\langle h(x), \nabla\cdot\rangle$-Operator to $X_\mu(\cdot, x_0)$.

In order to derive an efficient approximation of the stiffness matrix $\mathbf{A}$ from the approximation of the kernel, we have to define appropriate regions on the boundary surface Γ, such that the approximation error could be controlled by (6.2),(6.3). Let $\mathcal{P}(\Gamma)$ denote the set of all subsets of Γ and $\mathcal{C} \subset \mathcal{P}(\Gamma) \times \mathcal{P}(\Gamma)$ a finite set defining a partition of $\Gamma \times \Gamma$. The elements of the first and second component of $\mathcal{C}$, i.e.,

$$\mathcal{X} := \mathcal{X}_\mathcal{C} := \{\sigma \subset \Gamma : \exists\, \tau \subset \Gamma\,, (\sigma,\tau) \in \mathcal{C}\} \tag{6.8a}$$

$$\mathcal{Y} := \mathcal{Y}_\mathcal{C} := \{\tau \subset \Gamma : \exists\, \sigma \subset \Gamma\,, (\sigma,\tau) \in \mathcal{C}\}, \tag{6.8b}$$

are called clusters. A pair of clusters $(\sigma,\tau) \in \mathcal{C}$ is η-admissible, iff

$$\check{r}_\sigma + \check{r}_\tau \leq \eta |\check{c}_\sigma - \check{c}_\tau|, \tag{6.9}$$

where $\check{r}_M$ and $\check{c}_M$ denote for $M \subset \mathbb{R}^3$ the Čebyšev radius and center, respectively. Using this property we split the partition $\mathcal{C}$ into a *far field*

$$\mathcal{F} := \mathcal{F}_\mathcal{C}(\eta) := \{(\sigma,\tau) \in \mathcal{C} : (\sigma,\tau) \text{ is } \eta\text{-admissible}\} \tag{6.10}$$

and a *near field*

$$\mathcal{N} := \mathcal{N}_{\mathcal{C}}(\eta) := \mathcal{C} \backslash \mathcal{F}_{\mathcal{C}}(\eta) \tag{6.11}$$

which implies a corresponding splitting of the stiffness matrix $\mathbf{A}$ into a near field contribution $\mathbf{N}$ and a far field contribution $\mathbf{F}$:

$$(\mathbf{N})_{i,j} := \sum_{(\sigma,\tau)\in\mathcal{N}} \int_\sigma b_i(x) \int_\tau k(x,y)\, b_j(y)\, dydx \tag{6.12}$$

$$(\mathbf{F})_{i,j} := \sum_{(\sigma,\tau)\in\mathcal{F}} \int_\sigma b_i(x) \int_\tau k(x,y)\, b_j(y)\, dydx \tag{6.13}$$

Since the domains of integration of the far field part are well-separated, i.e., satisfy (6.3) with $x_0 := \check{c}_\sigma$ and $y_0 := \check{c}_\tau$, the kernel k can be replaced by its approximation k_m which in turn yields an approximation of $\mathbf{F}$:

$$\mathbf{F} \approx \sum_{(\sigma,\tau)\in\mathcal{F}} \mathbf{X}_\sigma \mathbf{F}_{\sigma\tau} \mathbf{Y}_\tau, \tag{6.14}$$

where the matrices $\mathbf{X}_\sigma$, $\mathbf{Y}_\tau$, and $\mathbf{F}_{\sigma\tau}$ are defined by

$$(\mathbf{X}_\sigma)_{i,\mu} := \int_\sigma b_i(x) X_\mu(x; c_\sigma) dx, \quad (\mathbf{Y}_\tau)_{\nu,j} := \int_\tau b_j(y) Y_\nu(y; c_\tau) dy \tag{6.15}$$

$$(\mathbf{F}_{\sigma\tau})_{\mu,\nu} := \begin{cases} \kappa_{\mu\nu} & \text{if } (\mu,\nu) \in \mathcal{I}_m \\ 0 & \text{else} \end{cases} \tag{6.16}$$

In other words, the stiffness matrix is approximated by a near field matrix $\mathbf{N}$ and a finite sum of rank-$|\mathcal{J}_m|$ modifications corresponding to the approximation of the kernel by degenerate kernels. The matrices $\mathbf{X}_\sigma$ only depend on x, the matrices $\mathbf{Y}_\tau$ only on y, and the matrices $\mathbf{F}_{\sigma\tau}$ contain the expansion coefficients $\kappa_{\mu\nu}$.

Essential for the efficiency of the algorithm is (i) the construction of a partition $\mathcal{C}$ such that the near field matrix $\mathbf{N}$ is a sparse matrix, i.e., contains only $O(N)$ entries, and (ii) the fast evaluation of the approximate far field contribution (6.14), in particular the fast evaluation of the matrix vector product

$$\mathbf{v} = \sum_{(\sigma,\tau)\in\mathcal{F}} \mathbf{X}_\sigma\, \mathbf{F}_{\sigma\tau} \mathbf{Y}_\tau\, \mathbf{u}. \tag{6.17}$$

The key is a hierarchical organization of clusters. Let $\mathcal{P}$ denote the given panelization of Γ. We subdivide $\mathcal{P}$ into two about equally large sets recursively until the subsets contain $O(1)$ panels. This defines a binary tree with root $\mathcal{P}$. Each node of the tree represents a subset of $\mathcal{P}$ which in turn implies a subset of Γ, i.e. the binary tree defines a hierarchical decomposition of Γ into clusters.

By traversing the tree a suitable partition $\mathcal{C} = \mathcal{F} \cup \mathcal{N}$ is constructed:

```
partition(σ, τ, F, N){
  if (σ is a leaf) or (τ is a leaf) then
    N ← {(σ, τ)} ∪ N
  else if ((σ, τ) η-admissible) then
    F ← {(σ, τ)} ∪ F
  else if (ř_σ < ř_τ) then
    for all children τ' of τ   partition(σ, τ', F, N)
  else
    for all children σ' of σ   partition(σ', τ, F, N)
}
```

The matrix vector product (6.17) is evaluated in three steps:

1. evaluate $\mathbf{u}_\tau := \mathbf{Y}_\tau \mathbf{u}$ for all $\tau \in \mathcal{Y}$,
2. evaluate $\mathbf{v}_\sigma := \begin{cases} \mathbf{F}_{\sigma\tau} u_\tau & \text{for } (\sigma,\tau) \in \mathcal{F}, \\ 0 & \text{otherwise} \end{cases}$ for all $\sigma \in \mathcal{X}$,
3. evaluate $\mathbf{v} = \sum_\sigma \mathbf{X}_\sigma \mathbf{v}_\sigma$.

The first and the last step could be accelerated by using so-called shift operations. We find

$$\mathbf{Y}_\tau = \sum_{\tau' \text{ child of } \tau} \mathbf{D}_{\tau\tau'} \mathbf{Y}_{\tau'}, \tag{6.18}$$

with matrices $\mathbf{D}_{\tau\tau'}$, i.e.,

$$\mathbf{u}_\tau = \begin{cases} \mathbf{Y}_\tau \mathbf{u} & \text{for } \tau \text{ a leaf}, \\ \sum_{\tau' \text{ child of } \tau} \mathbf{D}_{\tau\tau'} \mathbf{u}_{\tau'} & \text{otherwise}. \end{cases} \tag{6.19}$$

Hence, to evaluate $\mathbf{u}_\tau$ for all $\tau \in \mathcal{Y}$ we only have to assemble matrices $\mathbf{Y}_\tau$ if τ is a leaf. These matrices are sparse with $O(|\mathcal{J}_m|) = O(m^2)$ entries. The products $\mathbf{D}_{\tau\tau'}\mathbf{u}_{\tau'}$ are handled by efficient algorithms without assembling $\mathbf{D}_{\tau\tau'}$ explicitly [1]. The same holds for step 3. With matrices $C_{\sigma\sigma^*}$ defined by

$$\mathbf{X}_{\sigma^*} = \sum_{\sigma \text{ child of } \sigma^*} \mathbf{X}_\sigma \mathbf{C}_{\sigma\sigma^*}, \tag{6.20}$$

and vectors $\bar{\mathbf{v}}_\sigma := \mathbf{v}_\sigma + \mathbf{C}_{\sigma\sigma^*}\bar{\mathbf{v}}_{\sigma^*}$, σ child of σ^*, it follows that

$$\mathbf{v} = \sum_\sigma \mathbf{X}_\sigma \mathbf{v}_\sigma = \sum_{\sigma \text{ a leaf}} \mathbf{X}_\sigma \bar{\mathbf{v}}_\sigma. \tag{6.21}$$

Again, only matrices $\mathbf{X}_\sigma$ for leaves $\sigma \in \mathcal{X}$ must be assembled.

An analysis of the complexity (cf. [3], [12]) shows that the number of operations necessary to perform the matrix vector product (6.17) is of order $O(m^4 N)$, with N the number of unknowns.[1] The memory requirements are of order $O(m^2 N)$. To ensure that the error of the far field approximation is asymptotically equal to the order of the discretization error, we have to choose $m = O(\log\, N)$.

7 Numerical experiments

The main objective of the numerical experiment is (1) to validate the saddle point formulation, (2) to validate the clustering algorithm and (3) to validate the $O(N\log^4 N)$ complexity of the algorithm. In addition we want to demonstrate the performance of the method compared to the classical BEM algorithm in terms of CPU-time, storage requirement. Finally, we want to demonstrate that the fast algorithm is suited to solving geodetic boundary value problems. Rather than computing a full linearized Molodensky problem with real data, we chose two model problems, which nevertheless exhibits the most important features of the linearized Molodensky case, and therefore, allow addressing the items stated above.

In the first experiment we solve the following problem: The "true" potential is given by

$$U(x) = |x|^{-1} + x_1 x_2\, |x|^{-5} \tag{7.1}$$

and the embedding $\varphi = id$, i.e. $\Gamma = S^2$, and $h(x) = -n(x)$ with $n(x)$ the exterior unit normal vector to Γ.

The main difference between this problem and the linearized vector Molodensky problem (2.1) is the spherical geometry and the boundary operator which involves the normal derivative instead of the oblique derivative. However, our approach does rely neither on the normal derivative nor on the spherical geometry of the boundary surface. In fact, the saddle point formulation and the fast algorithm are applicable without any modification for oblique derivative problems and non-spherical geometries, as well. The decision to use $\varphi = id$ and $h(x) = -n(x)$ has been done for reasons of simplicity.

We approximated the unit sphere by planar triangles. Continuous piecewise linear polynomials have been used as trial and test functions. The numerical quadrature for the near field integrals has been done using special quadrature techniques [9],[7].

[1] With a more sophisticated approach to evaluate the products $\mathbf{F}_{\sigma\tau}\mathbf{u}_\tau$ using exponential expansions this could be reduced to $O(m^3 N)$ [1].

The linear system of equations (LSE) was solved using a GMRES solver without any preconditioning. About 30 iterations were necessary to keep the error lower than the discretization error, independent of the number of unknowns. For our cluster algorithm the matrix-vector operations for the calculation of the far field contribution have been done in every iteration step. The necessary information about the $\mathbf{X}_\sigma$, $\mathbf{Y}_\tau$ and $\mathbf{F}_{\sigma\tau}$ matrices have been stored in core on the workstation. The quality of the solution has been checked at a grid of points with distance 0.5 to the surface of the unit sphere.

The results were obtained on a *SUN* Ultra-Enterprise 4000/5000 on a single processor (*UltraSPARC*, 248MHz), 2 GB RAM using the *SUN* C++ 4.2 Compiler and the class library *Concepts-1.3* for boundary elements.

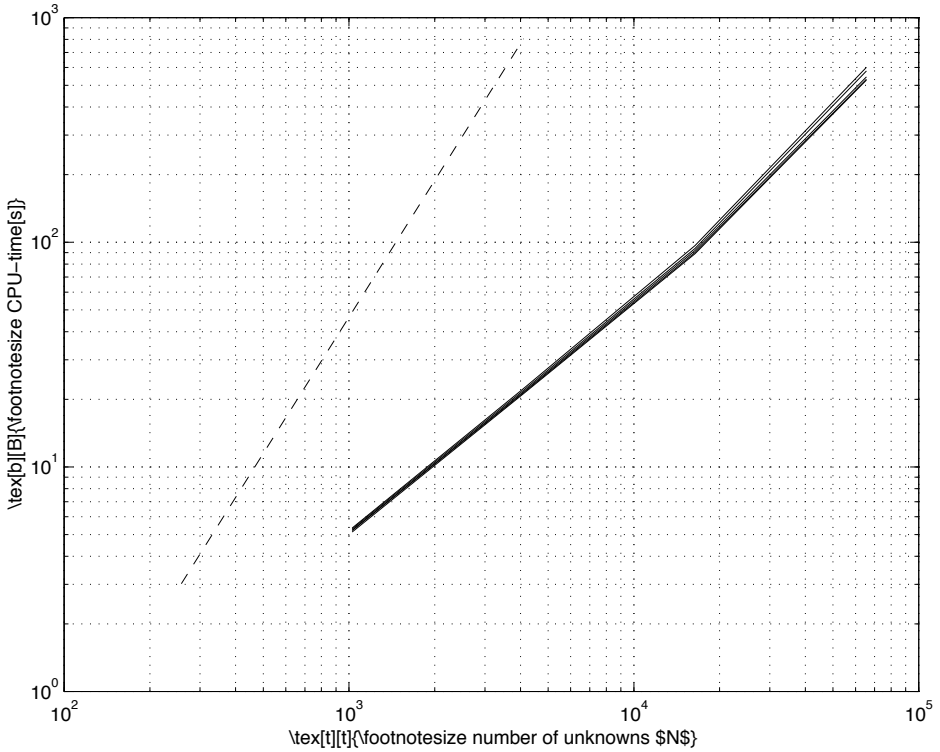

Figure 1: CPU-time for matrix assembly ($m = 3, 4, 5, 6, 7$)(in seconds) versus number N of panels: standard BEM (dashed line) versus fast algorithm (solid lines).

Figure 1 shows the CPU-time for the matrix assembly for the standard BEM (dashed line) and our fast algorithm (solid lines). The latter depends on the order m of the multipole expansion. The computations have been done for $m = 3 \ldots 7$. The results are shown as function of the number of unknowns, i.e., of the resolution. At the finest resolution (65538 unknowns, 131072 panels) the (spherical) distance between the data points is smaller than 1.1 degrees. This corresponds to a global solution in terms of spherical harmonics up to

degree and order 360 (half-wavelength resolution 0.5 degrees), since we used linear trial functions. The dependence on m is minor, because N dominates. Compared with the standard method a speed-up of up to 3 orders of magnitude can be expected for the finest resolution.

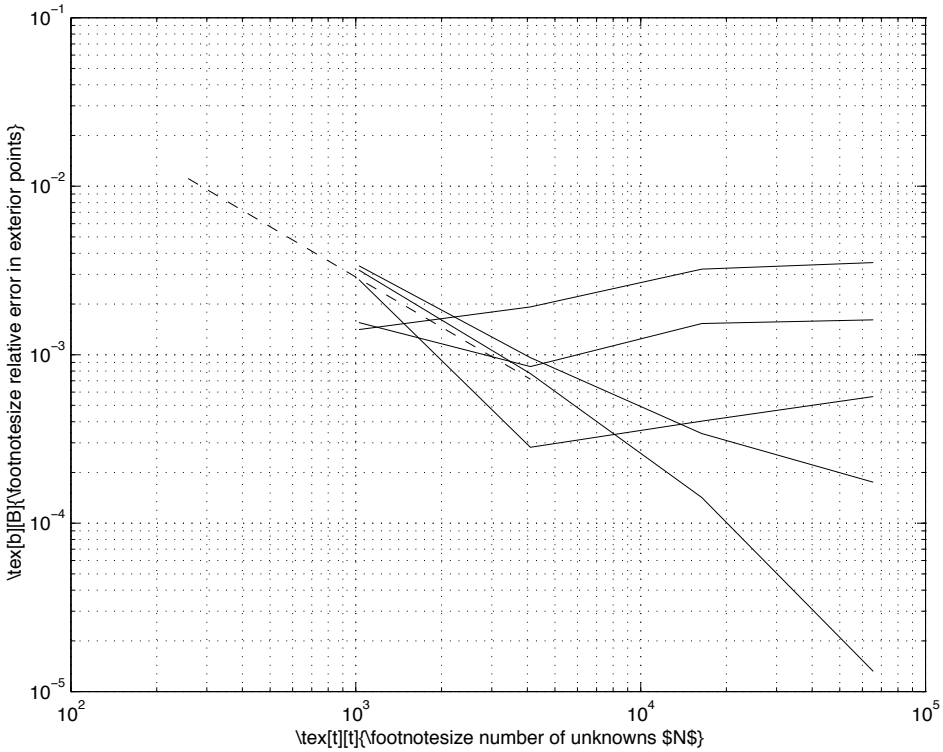

Figure 2: Relative mean absolute error in a set of points with distance 0.5 from the surface of the unit sphere versus the number of panels: standard BEM (dashed line) versus fast algorithm for $m = 3, 4, 5, 6, 7$ (solid lines).

Figure 2 shows the relative mean absolute error in the potential in exterior points located at a distance of 0.5 from the surface of the unit sphere. The solid lines represent the cluster-BEM solution for $m = 3 \ldots 7$, the dashed line represents the standard-BEM solution. Only for $m = 6, 7$ we observe an almost monotone decreasing error with increasing number of unknowns. This indicates that small values of m corresponding to low expansion orders produce approximation errors that dominate the total error budget if the discretization becomes finer. At a certain discretization level $m = 5$ gives a better accuracy than $m = 7$. This can be explained by the influence of the discretization error which dominates at this discretization level the total error budget. Therefore, variations in order of the discretization error can be expected.

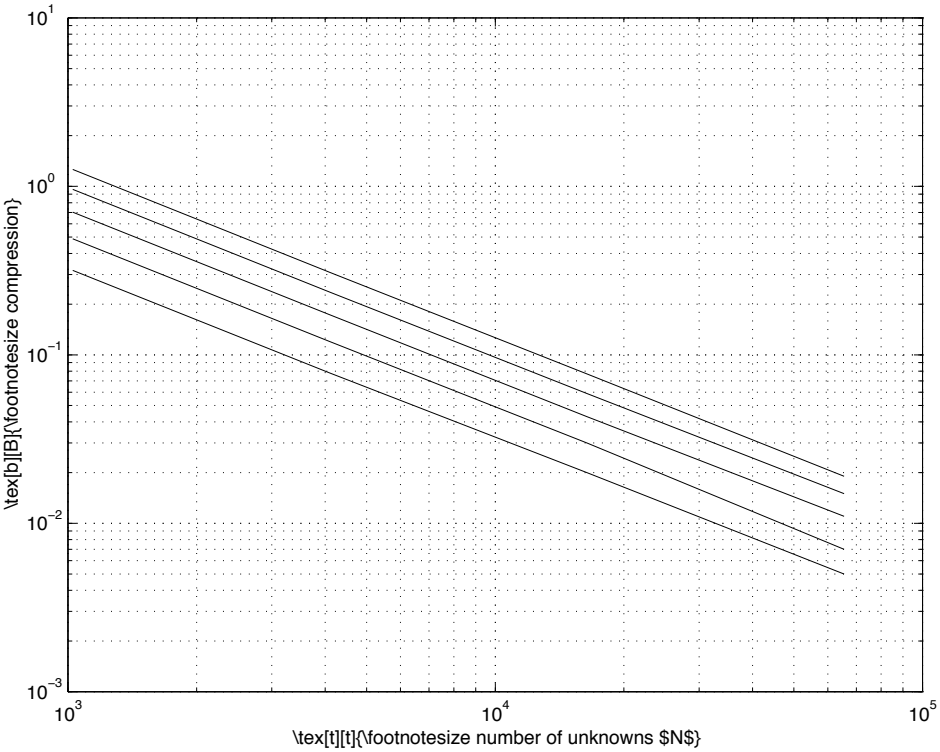

Figure 3: Compression of the stiffness matrix for $m = 3, 4, 5, 6, 7$ versus the number of panels.

Figure 3 shows the compression rate as a function of the number of unknowns. A compression factor of 0.01 means that the total of entries to store the necessary information of the $\mathbf{X}_\sigma$, $\mathbf{F}_{\sigma\tau}$, $\mathbf{Y}_\tau$ matrices is equal to 1% of the entries of the dense stiffness matrix $\mathbf{A}$.

In Figure 4 we show the number of necessary matrix entries for the cluster-BEM and the standard-BEM as a function of the potential error in exterior points. It clearly shows that the higher the accuracy requirements are the more storage could be saved with the cluster-BEM.

In the second test we used the IAG Earth Model developed in the framework of the IAG Working Group on "Numerical Techniques for Geodetic Boundary Value Problems" within Special Commission 1 of Section IV [2]. The boundary value problem we solved is the Robin problem

$$\begin{aligned} \triangle T(x) &= 0 \qquad && x \in \text{ext } \Gamma \\ -\frac{1}{R}T(x) + \frac{\partial T}{\partial n} &= f(x) && x \in \Gamma \\ T(x) &\to 0, && |x| \to \infty. \end{aligned} \tag{7.2}$$

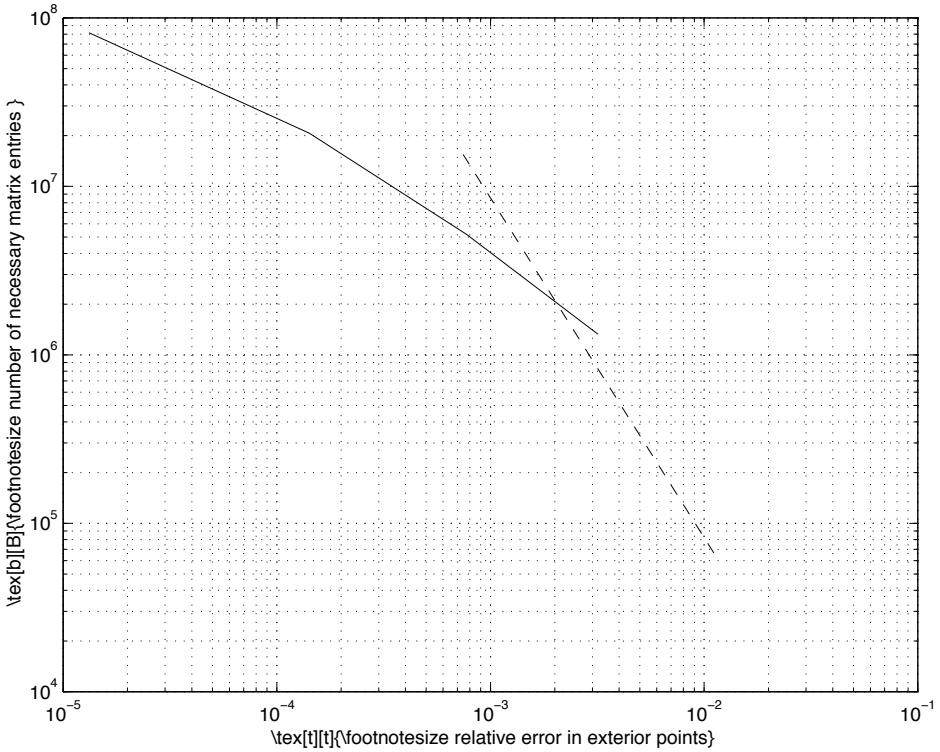

Figure 4: Number of necessary matrix entries as function of the potential error in exterior points: standard BEM (dashed line) versus fast algorithm ($m = 7$) (solid line).

R is the mean radius of the Earth. The boundary surface Γ is very similar to the topography of the Earth as described by the GETECH topography model. The synthetic gravity field was generated with a maximum resolution of approximtely 750 km [2]. See Figure 6 for a picture of the boundary data for the BVP computed from this field. This field resembles as closely as possible the true gravity field of the earth but filtered such that its content can be represented by the sampling points of the level 4 triangulation, which have a maximal distance of 8.7 degrees. In addition, the signal does not contain the zero and first oder term.

The triangulation of the topography is based on a subsequent subdivision of the triangular faces of an octahedron. Each of the eight faces of the octahedron is first subdivided into 4 congruent subtriangles by halving the sides. This defines the triangles at level 1. The process is repeated until the maximum level is reached. At level l there are $8 \cdot 4^l$ triangles. The projection of the corners of the triangles ('nodes') onto the topography defines the corners of the triangulation of the topography (see figure 5). Finally, the boundary data have been generated at these corners. No noise has been added. Table 1 contains for level $4 - 7$ the number of triangles, the number of nodes (data points) and the minimum

Level	Triangles	Nodes	Res. (deg.)
4	2048	1026	8.7
5	8192	4098	4.4
6	32768	16386	2.2
7	131072	65538	1.1

Table 1: Number of elemenents and minimum resolution for each level.

resolution.

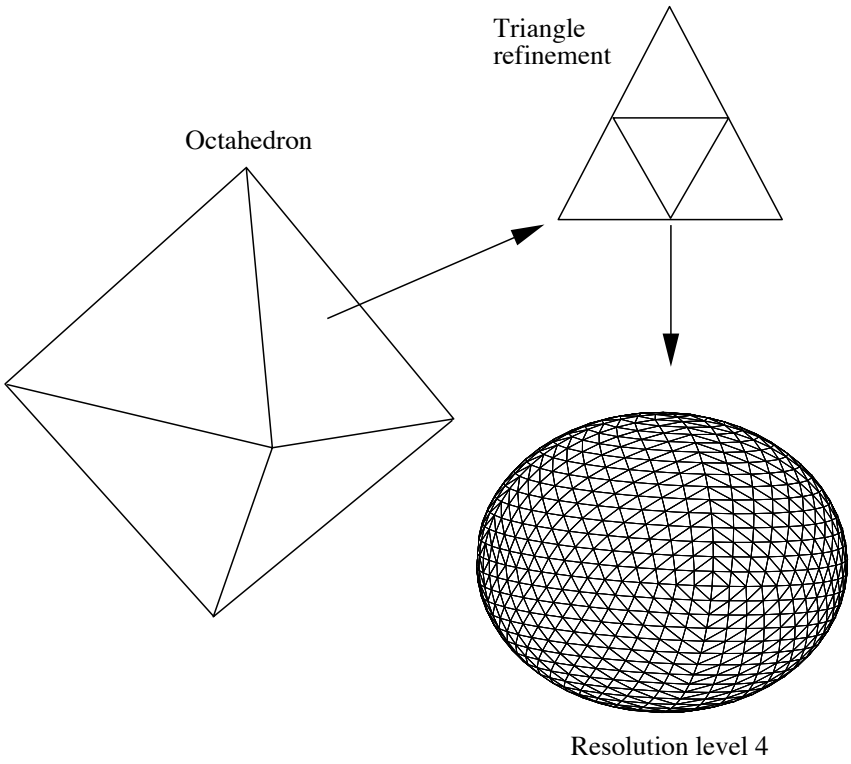

Figure 5: The panel subdivision.

The computations have been done on a HP-C180 workstation with 512 Mb internal memory. Due to memory constraints the simulations were only carried out up to level 6. The results for higher levels were obtained by extrapolation. They are indicated in Figures 7- 10 by dashed lines. The maximum distance between the data points at level 6 is about 2.2 degree. Since piecewise linear polynomials have been used as trial functions, the maximum resolution of the trial space is about one level higher. Therefore, a level-7 solution represents similar details as a spherical harmonic expansion up to degree and order 360. The performance in terms of the CPU-time for matrix assembly and for the solution of the

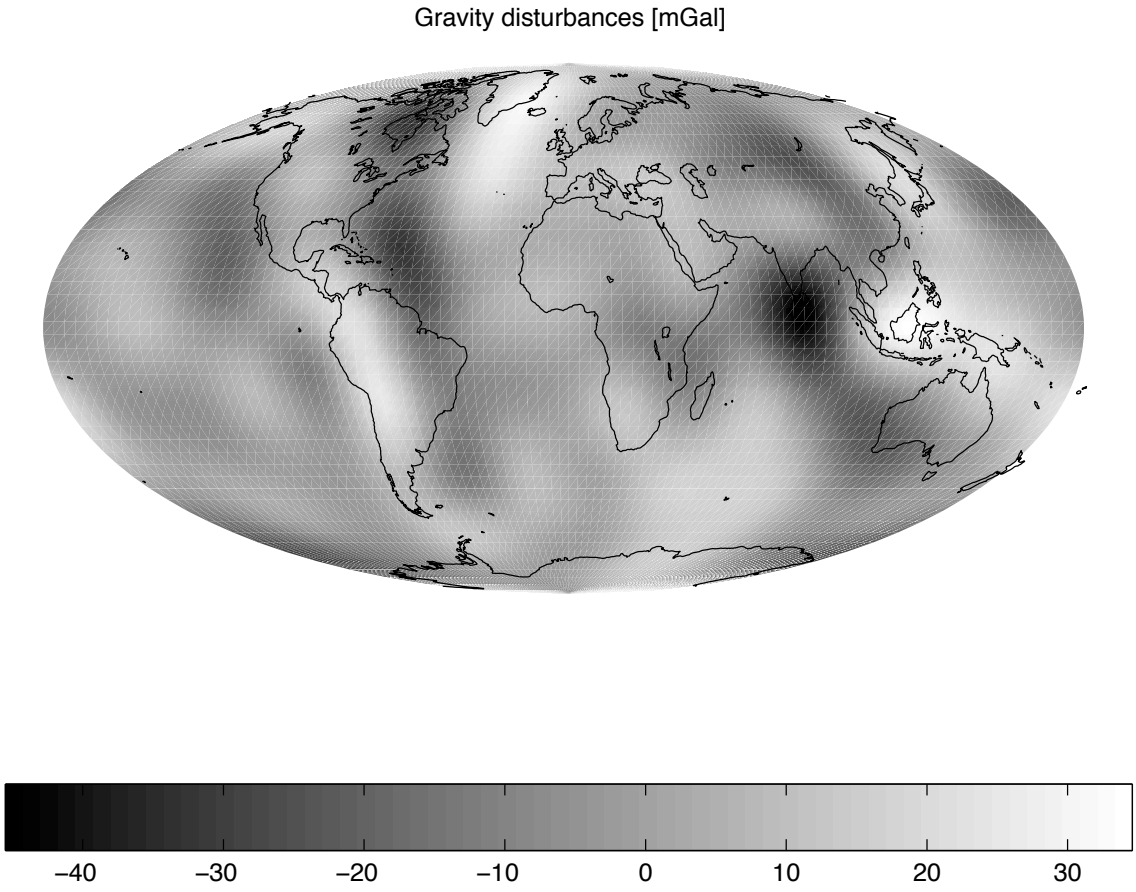

Figure 6: The boundary data (no zero- and first-degree terms).

linear system of equations is comparable to the first test (cf. Figure 7, 8). The storage requirements for the standard BEM algorithm increase very fast with higher levels. Due to the efficient approximation of the matrix-vector product **Fu**, which is the basic operation in the GMRES algorithm, much memory can be saved with the fast algorithm: up to two orders of magnitude for level 7, depending on the order m of the cluster expansion (see Figure 9). The results shown for $m = 3$ and $m = 6$ indicate that the storage requirements increase with increasing degree of the multipole expansion. Theoretically, the increase is proportional to m^2, which may cause a problem for large m. The actual choice of m depends on the dimension N of the solution space. We have to choose $m = O(\log N)$ in order to keep the error due to the degenerate kernel approximation below the error of the Galerkin discretization.

We also studied the accuracy of the BEM solution at external data points. We selected test points at a height of $1.5 \times R$ above the corner points of the level 4 triangulation, where R is the Earth's mean radius. We computed the mean square difference "true -

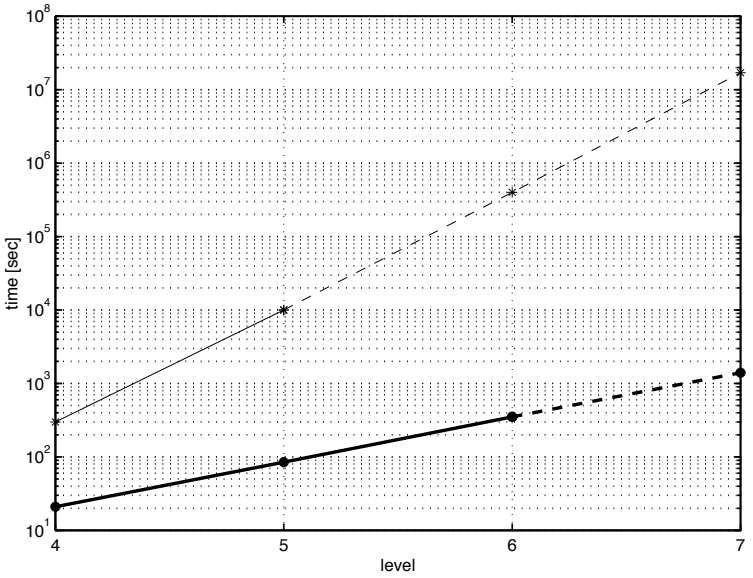

Figure 7: The CPU time (seconds) for stiffness matrix assembly (bold: fast algorithm, m=3; normal: standard BEM algorithm)

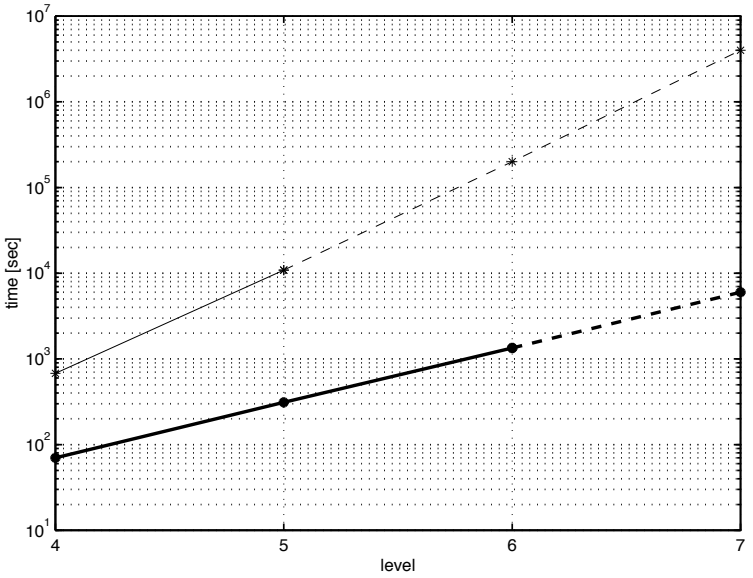

Figure 8: The CPU time (seconds) for stiffness matrix assembly and solution of the linear system of equations (bold: fast algorithm, m=3; normal: standard BEM algorithm.

computed" of the disturbing potential at these points. The results are shown in Figure 10. We observe a significant improvement for higher levels although the improvement is not

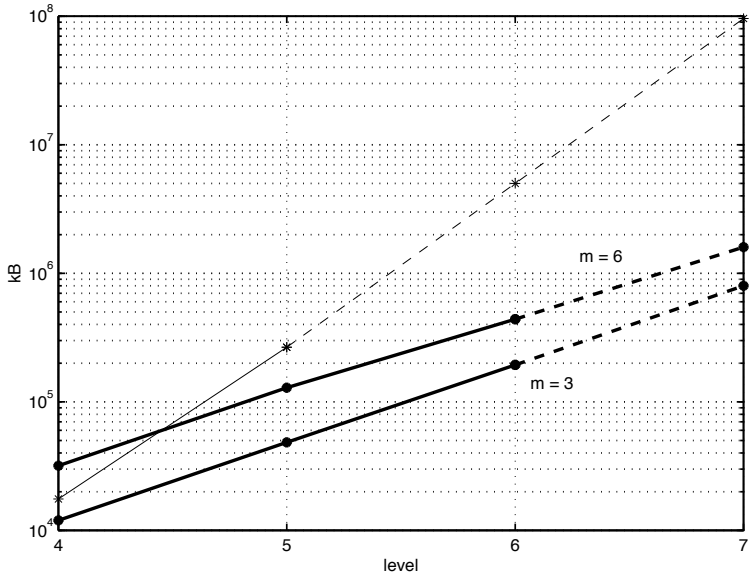

Figure 9: Storage requirements (bold: fast algorithm; normal: standard BEM algorithm).

steady when augmenting the level. At level 6 the relative mean square potential difference is about $8.9 \cdot 10^{-4}$. Please note that the error reflects the sum of the discretization error, the error of numerical integration, and the error of kernel approximation.

8 Perspectives for physical geodesy

The saddle point formulation and the fast algorithm are well-suited for solving geodetic BVPs. The former guarantees not only the well-posedness of the discrete problem but also allows to properly include any a priori given geopotential models. This is an essential requirement since the most accurate long wavelength geopotential models (up to degree and order, say, 50 of a spherical harmonic expansion) obtained so far are derived from satellite observations. Most of these coefficients cannot be improved from terrestrial data, and, therefore, have to be fixed in the solution of the Molodensky boundary value problem as has been shown in [6] and [10]. In the near future dedicated satellite gravity field missions such as the German CHAMP, the US/German GRACE and ESA's GOCE will provide even medium wavelengths with unprecedented accuracy. Then, terrestrial data will provide locally improved gravity field solutions with resolutions of, say, 5×5 minutes for areas as large as Europe and North America; comparable resolutions may also be computed for the oceans.

The fast boundary element algorithm has the potential to speed up the assembly and

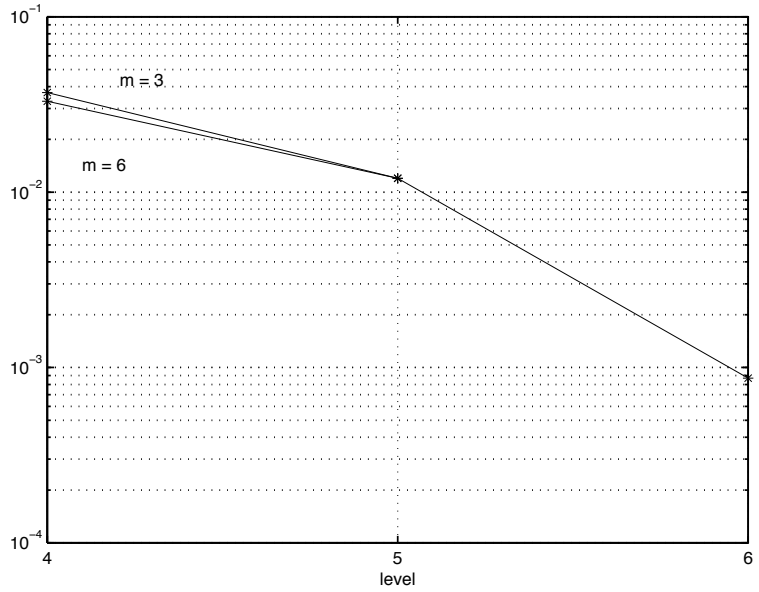

Figure 10: Relative mean square difference "true-computed" at evenly distributed control points with distance $1.5 \times R$ above the surface (R mean Earth's radius). Do to memory constraints $m = 6$ has been computed for level 4 and 5 only.

solution of the linear system by $2 - 3$ orders of magnitude, and to reduce the storage requirements by about the same amount. Therefore, it will make high resolution global and local gravity field recovery feasible. The flexibility and efficiency of our method should not degrade significantly if oblique derivatives are taken into account, or if a large number of geopotential coefficients has to be fixed, and if higher order gravity fields have to be recovered from terrestrial data. However, in order to assess this more numerical investigations have to be done. A major point of concern may be the m-term in the complexity estimates, which is of the order $O(\log N)$. When $m^4 \approx N$ for a reasonable choice of η, the number of operations necessary to perform the matrix-vector product is not significantly smaller than for the standard BEM algorithm. This would seriously degrade the performance of the fast algorithm. Similar statements hold for the memory requirements, which increase proportionally to m^2. The second numerical test, however, seems to indicate that even for a resolution equivalent to degree and order 360 the choice $m = 6$ may be sufficient, i.e. $m^4 \ll N$. However, before a definite answer can be given, more numerical tests have to be carried out. As far as ultra-high resolution local gravity field improvements are concerned, we are still missing a detailed error analysis for this type of *local* boundary value problems. Here local refinement and adaptivity afforded by the BEM may be attractive alternatives.

Acknowledgement: Roger Haagmans developed and implemented the synthetic earth

model we used in our test computations, and provided the boundary data and the control data. His support is gratefully acknowledged.

A Appendix

Here we supply the proof that the condition (2.1c) of vanishing $O(|x|^{-2})$-terms in the far-field expansion of U is equivalent to the orthogonality of the single layer density u to the restriction to the boundary Γ of the homogeneous harmonic polynomials of degree 1.

If U does not contain terms of order $O(|x|^{-2})$ then U is orthogonal to all surface spherical harmonics of degree 1 on any Brouillon sphere, i.e., on any surface S_R of a sphere of radius R and center 0 enclosing Γ:

$$\langle U, Y_{1,m'}\rangle_{L^2(S_R)} = \int_{S_R} U(x)\, Y_{1,m'}\left(\frac{x}{|x|}\right) dS_R(x) = 0, \qquad m' = -1, 0, 1, \tag{A.1}$$

where $\{Y_{1,m'} : m' = -1, 0, 1\}$ denotes the set of complex surface spherical harmonics of degree 1. For $x \in \operatorname{ext}\Gamma$, we may represent U by the single layer potential with density u:

$$U(x) = \int_\Gamma u(y)\, \frac{1}{|x-y|}\, d\Gamma(y), \qquad x \in \operatorname{ext}\Gamma. \tag{A.2}$$

Inserting (A.2) into (A.1) yields

$$\begin{aligned}\int_{x\in S_R} &\left(\int_{y\in\Gamma} u(y)\frac{1}{|x-y|}\, d\Gamma(y)\right) Y_{1,m'}\left(\frac{x}{|x|}\right) dS_R(x) \\ &= \int_{y\in\Gamma} u(y) \int_{x\in S_R} \frac{1}{|x-y|}\, Y_{1,m'}\left(\frac{x}{|x|}\right) dS_R(x)\, d\Gamma(y) = 0, \qquad m' = -1, 0, 1.\end{aligned}$$

Since

$$\frac{1}{|x-y|} = \sum_{n=0}^{\infty}\sum_{m=-n}^{n} (-1)^m \frac{|y|^n}{|x|^{n+1}}\, Y_{n,-m}\left(\frac{x}{|x|}\right) Y_{n,m}\left(\frac{y}{|y|}\right), \qquad \forall\ |x| > |y|,$$

we obtain

$$\begin{aligned}\sum_{n=0}^{\infty}\sum_{m=-n}^{n} &(-1)^m \int_{y\in\Gamma} u(y)\, |y|^n\, Y_{n,m}\left(\frac{y}{|y|}\right) \\ &\cdot \frac{1}{R^{n+1}} \int_{x\in S_R} Y_{n,-m}\left(\frac{x}{|x|}\right) Y_{1,m'}\left(\frac{x}{|x|}\right) dS_R(x)\, d\Gamma(y) = 0, \qquad m' = -1, 0, 1,\end{aligned} \tag{A.3}$$

where we have used that $|x| = R$, $\forall x \in S_R$. Observing the orthogonality property of the complex surface spherical harmonics,

$$\int_{S_R} Y_{n,-m}\, Y_{1,m'}\, dS_R = \frac{4\pi R^2}{3}(-1)^{m'}\delta_{mm'}\delta_{n1},$$

(A.3) is equivalent to

$$\int_{y\in\Gamma} u(y)\,|y| Y_{1,m'}\left(\frac{y}{|y|}\right) = 0, \qquad m' = -1, 0, 1. \tag{A.4}$$

$H_{1,m'} := |y|\, Y_{1,m'}\left(\frac{y}{|y|}\right)$ is a homogeneous harmonic polynomial of degree 1 and order m'. The space of homogeneous harmonic polynomials of degree 1 has dimension 3, so (A.1) is equivalent to

$$\langle u,\, H_{1,m'}|_\Gamma\rangle = 0, \qquad m' = -1, 0, 1,$$

i.e., u is orthogonal to the restriction to the boundary Γ of all homogeneous harmonic polynomials of degree 1. This completes the proof.

References

[1] L. Greengard and V. Rokhlin. A new version of the fast multipole method for the laplace equation in three dimensions. In Iserles A., editor, *Volume 6*, Acta Numerica, pages 229–269. Cambridge University Press, 1997.

[2] R. Haagmans. A synthetic earth model for use in geodesy. Submitted for publication.

[3] W. Hackbusch and Z.P. Nowak. On the Fast Matrix Multiplication in the Boundary Element Method by Panel Clustering. *Numerische Mathematik*, 54(4):463–491, 1989.

[4] S. Hildebrandt and E. Wienholtz. Constructive proofs of representation theorems in separable Hilbert spaces. *Comm. and Pure Appl. Math.*, 17:369–373, 1964.

[5] L. Hörmander. The boundary problems of physical geodesy. *Arch. Rat. Mech. Anal.*, 1976.

[6] R. Klees and R. Lehmann. Integration of a priori gravity field models in boundary element formulations to geodetic boundary value problems. In *Accepted for publication in Proc. IV Hotine-Marussi Symposium on Mathematical Geodesy, Trento, Italy*, 1999.

[7] Ch. Lage. *Softwareentwicklung zur Randelementmethode: Analyse und Entwurf effizienter Techniken*. PhD thesis, Universität Kiel, 1996. In german.

[8] Ch. Lage. Fast evaluation of singular kernel functions by cluster methods. Technical report, Seminar für Angewandte Mathematik, ETH Zürich, CH-8092 Zürich, 1998. In preparation.

[9] Ch. Lage and S. A. Sauter. Transformation of hypersingular integrals and black-box cubature. *Math. Comp.* To appear.

[10] R. Lehmann and R. Klees. Numerical solutions of geodetic boundary value problems using a higher degree reference field. *Accepted for publication in Journal of Geodesy*, 1999.

[11] A. Rathsfeld. *A wavelet algorithm for the boundary element solution of a geodetic boundary value problem*. Preprint 225, WIAS Berlin, 1997.

[12] V. Rokhlin. Rapid solutions of integral equations of classical potential theory. *J. Comput. Phys.*, 60:187–207, 1985.

[13] T. von Petersdorff and Ch. Schwab. Fully discrete multiscale Galerkin BEM. In W. Dahmen, P. Kurdila, and P. Oswald, editors, *Multiresolution Analysis and Partial Differential Equations*, Wavelet Analysis and its Applications, pages 287–346. Academic Press, 1997.

Research Reports

No.	Authors	Title
99-16	R. Klees, M. van Gelderen, C. Lage, C. Schwab	Fast numerical solution of the linearized Molodensky problem
99-15	J.M. Melenk, K. Gerdes, C. Schwab	Fully Discrete *hp*-Finite Elements: Fast Quadrature
99-14	E. Süli, P. Houston, C. Schwab	*hp*-Finite Element Methods for Hyperbolic Problems
99-13	E. Süli, C. Schwab, P. Houston	*hp*-DGFEM for Partial Differential Equations with Nonnegative Characteristic Form
99-12	K. Nipp	Numerical integration of differential algebraic systems and invariant manifolds
99-11	C. Lage, C. Schwab	Advanced boundary element algorithms
99-10	D. Schötzau, C. Schwab	Exponential Convergence in a Galerkin Least Squares *hp*-FEM for Stokes Flow
99-09	A.M. Matache, C. Schwab	Homogenization via *p*-FEM for Problems with Microstructure
99-08	D. Braess, C. Schwab	Approximation on Simplices with respect to Weighted Sobolev Norms
99-07	M. Feistauer, C. Schwab	Coupled Problems for Viscous Incompressible Flow in Exterior Domains
99-06	J. Maurer, M. Fey	A Scale-Residual Model for Large-Eddy Simulation
99-05	M.J. Grote	Am Rande des Unendlichen: Numerische Verfahren für unbegrenzte Gebiete
99-04	D. Schötzau, C. Schwab	Time Discretization of Parabolic Problems by the hp-Version of the Discontinuous Galerkin Finite Element Method
99-03	S.A. Zimmermann	The Method of Transport for the Euler Equations Written as a Kinetic Scheme
99-02	M.J. Grote, A.J. Majda	Crude Closure for Flow with Topography Through Large Scale Statistical Theory
99-01	A.M. Matache, I. Babuška, C. Schwab	Generalized *p*-FEM in Homogenization
98-10	J.M. Melenk, C. Schwab	The *hp* Streamline Diffusion Finite Element Method for Convection Dominated Problems in one Space Dimension
98-09	M.J. Grote	Nonreflecting Boundary Conditions For Electromagnetic Scattering
98-08	M.J. Grote, J.B. Keller	Exact Nonreflecting Boundary Condition For Elastic Waves
98-07	C. Lage	Concept Oriented Design of Numerical Software